Cancer Medicine

Open Access

ORIGINAL RESEARCH

Hyperbaric oxygen therapy sensitizes nimustine treatment for glioma in mice

Zhaohui Lu[1,a], Jiawei Ma[1,a], Bing Liu[1], Chungang Dai[1], Tao Xie[1], Xiaoyu Ma[1], Ming Li[2], Jun Dong[1], Qing Lan[1] & Qiang Huang[1]

[1]Department of Neurosurgery, The Second Affiliated Hospital of Soochow University, 1055 Sanxiang Rd, Suzhou 215004, China
[2]The Experimental Center, The Second Affiliated Hospital of Soochow University, 1055 Sanxiang Rd, Suzhou 215004, China

Keywords
Chemotherapy, glioma stem cell, green fluorescence transgenic nude mice, hyperbaric oxygen therapy, immunity inflammation, transplantation model

Correspondence
Jun Dong, Department of Neurosurgery, The Second Affiliated Hospital of Soochow University, 1055 Sanxiang Rd, Suzhou 215004, China. Tel/Fax: +8613962157301; E-mail: dongjun@suda.edu.cn

Funding Information
This study was supported by grants from the National Natural Science Foundation (81472739, 81572480, 81172400), the Natural Science Foundation of Jiangsu China (BK20151214), and the Suzhou Science and Technology Development Program (SYS201507).

Received: 18 March 2016; Revised: 10 July 2016; Accepted: 13 July 2016

***Cancer Medicine* 2016; 5(11):3147–3155**

doi: 10.1002/cam4.851

[a]These authors contributed equally to the work.

Abstract

Nimustine (ACNU) has antitumor activities in patients with malignant glioma. Hyperbaric oxygen (HBO) may enhance the efficacy of certain therapies that are hampered by the hypoxic microenvironment. We examined the combined effects of ACNU and HBO in a GFP transgenic nude mice bearing human glioma model. Mice inoculated with human glioma cells SU3 were randomly divided into the four groups: (A) the control group, (B) the HBOT (HBO therapy) group, (C) the ACNU group, and (D) the HBOT+ACNU group. Tumor size was measured at the indicated time intervals with a caliper; mice were sacrificed 28 days after treatment, and immunohistochemistry staining and western blot analysis were carried out. By the end of the trial, the tumor weights of groups A, B, C, and D were ($P < 0.05$), 6.03 ± 1.47, 4.13 ± 1.82 ($P < 0.05$), 2.39 ± 0.25 ($P < 0.05$), and 1.43 ± 0.38 ($P < 0.01$), respectively. The expressions of TNF-α, MMP9, HIF-α, VEGF, NF-κB, and IL-1β were associated with the infiltration of inflammatory cells and the inhibition rate of tumor cells. Hyperbaric oxygen therapy (HBOT) could inhibit glioma cell proliferation and inflammatory cell infiltration, and exert a sensitizing effect on ACNU therapy partially through enhancing oxygen pressure (PO_2) in tumor tissues and lower expression levels of HIF-1α, TNF-α, IL-1β, VEGF, MMP9, and NF-κB.

Introduction

Hyperbaric oxygen therapy, the noninvasion treatment, has been widely used in many common diseases, such as carbon monoxide poisoning. Almost all the hypoxic diseases were adaptive [1], however, there had been debates over HBO therapy for cancer patients in the past few decades [2, 3]. By using the HBO therapy in mice bearing tumor, Stuhr et al. [4] proposed that hyperbaric oxygen might inhibit the growth of glioma cells, subcutaneously transplanted in C57BL/6J mice. It had been reported that HBOT combined with 5-FU and doxorubicin had increased sensitivity in the treatment of solid tumors in mice [5, 6]. However, HBOT did accelerate tumor's growth [7]. And it was showed that HBOT promoted the pulmonary metastasis of breast cancer of C3H mouse [8].

The reasons for the debate were difficult to distinguish. It was believed that the HBO therapy efficacy might be tumor cell-type specific. In this report, the glioma-bearing animals were treated with HBOT, ACNU, or the combination of both. The whole experiment was carried in the fully closed and individual ventilated cages (IVC), which

guaranteed that the nude mice lived in SPF environment, and were not affected by HBOT. We found that the hyperbaric oxygen therapy significantly increased the sensitivity of nimustine treatment for mice bearing glioma.

Material and Methods

Mice and reagents

The human glioma stem/progenitor cell line SU3 and nude mice expressing EGFP (NC-CB57/6J-EGFP) were prepared by our laboratory [9, 10]. The NC-C57BL6J-EGFP mice (6–8 weeks of age) were established by our group and maintained in independent ventilation cages. The independent ventilated cage barrier system used in the feeding room and in the hyperbaric oxygen cabin was developed jointly with Suzhou Suhang Science & Technology Co., Ltd. (Jiangsu China) (Fig. 1). Hyperbaric oxygen chamber was purchased from Ningbo Medical Hyperbaic Oxygen Chamber Factory (Zhejiang China). Nimustine was purchased from Daiichi Sankyo Company Ltd. (Beijing China). Fluorescence microscope was purchased from Carl Zeiss (Shanghai China). HIF-α, VEGF, MMP9, NF-κB, and TNF-α antibodies were purchased from Abcam. (USA). IL-1β antibody was purchased from Cell Signaling Technology (USA).

Mouse model

The mice used in this study were aged 6–8 weeks and had a body weight of ~22 g. All the mice were bred and maintained in the specific pathogen-free animal care facility. SU3 cells (5×10^6 cells in 80 μL of PBS) were subcutaneously injected in the flank of the nude mice. The mice were divided into the four groups randomly: (A) control group (untreated), (B) HBOT (only), (C) ACNU (only), (D) HBOT+ACNU (combination). Each group had five mice. All treatments were initiated on day 8, when the tumor size reached 40–60 mm^3. HBO was administrated daily for 3 weeks. ACNU (3 mg/kg; i.p.) was administered once per week for 3 weeks. Tumor size was measured twice per week using a digital caliper, and tumor volume (V) was calculated using the formula $V = [1/2]ab^2$, where a and b were the long and short diameters of the tumor, respectively. Mice were sacrificed 4 weeks postinjection, following which tumors were carefully removed, and their weight and tumor volume were measured prior to further histological evaluation.

Hyperbaric oxygen treatment

Mice in the hyperbaric oxygen treatment group were placed into a homemade device for hyperbaric oxygen therapy

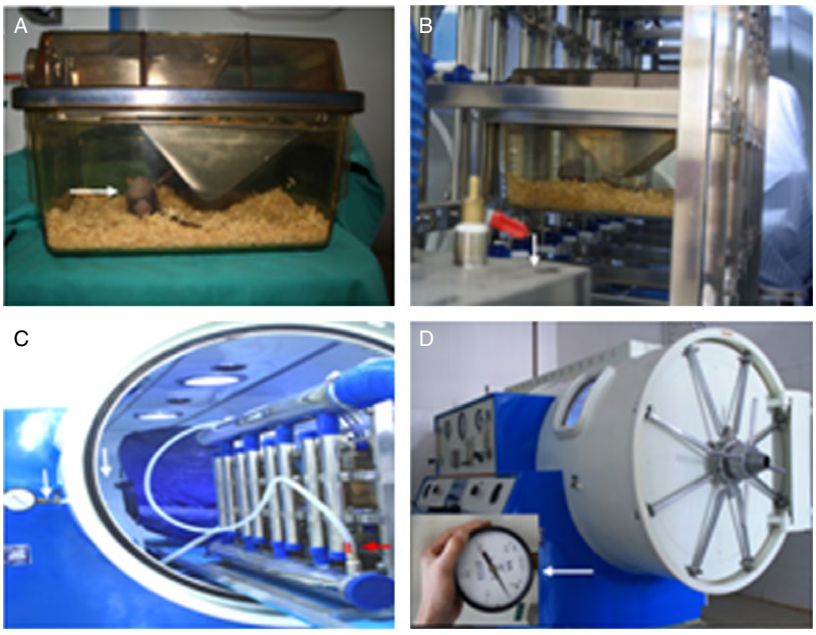

Figure 1. Hyperbaric oxygen—individual-ventilated cage (HBO-IVC) system. (A) A tumor-bearing mouse (arrow) inside the IVC; (B) fully enclosed transport channel and the air filter apparatus (arrow) connecting the feeding room to the hyperbaric oxygen therapy (HBOT) room; (C) standby HBO-IVC with plastic hose connecting the exhaust manifold (red arrow) and the pressure valve (white arrow) on the window; (D) working HBO-IVC with manometer monitoring the pressure inside IVC. The mice were divided into the four groups randomly, and each group had five mice, as shown in the Material and Methods section.

(specific pathogen-free level was kept; Fig. 1). HBO was administered at a pressure of 2.5 atm for 90 min. A minimum of 15 min pressurization and depressurization was allowed for the nude mice to adjust to the changes in pressure. The treatment regimen consisted of a 5–10 min ramp-up to 2.5 atm pressure in a 100% O_2 environment, followed by sustaining for 90 min at this pressure prior to a 10- to 20-min decompression phase. The hyperbaric oxygen intervention process was performed daily for 21 days.

Immunohistochemistry

Tumor tissue blocks were cut into 4 μm sections, which were incubated with rabbit polyclonal anti-HIF1α (diluted 1:250), rabbit polyclonal anti-VEGF (diluted 1:250), rabbit polyclonal anti-mmp9 (diluted 1:200), rabbit polyclonal anti-IL-1β (diluted 1:10), rabbit polyclonal anti-NF-κB (diluted 1:100), or rabbit polyclonal anti-TNF-α (diluted 1:150) at 4°C overnight in humid champers. Sections were observed under a laser confocal scanning microscope at a magnification of 400×. Immunohistochemical staining was quantitated using IPP 6.0 image analysis software (Media Cybernetics, USA), and 5–8 fields of view were selected on each section and photographed. Image analyses were performed as described, and mean optical density (MOD) were calculated using the following formula: MOD = Integral optical density/area of interest. MOD was obtained for the various fields of view in each section.

Western blot analysis

Tumor tissues were cut into pieces, rinsed twice with ice-cold PBS, and solubilized in lysis buffer containing 20 mmol/L Tris (pH 7.5), 135 mmol/L NaCl, 2 mmol/L EDTA, 2 mmol/L DTT, 25 mmol/L β-glycerophosphate, 2 mmol/L sodium pyrophosphate, 10% glycerol, 1% Triton X-100, 1 mmol/L sodium orthovanadate, 10 mmol/L NaF, 10 μg/mL aprotinin, 10 μg/mL leupeptin, and 1 mmol/L phenylmethylsulfonyl fluoride (PMSF) for 30 min. Lysates were centrifuged (15,000*g*) at 4°C for 15 min. Equal amounts of the soluble proteins were denatured in SDS, electrophoresed on a 12% SDS-polyacrylamide gel, and transferred to a polyvinylidene difluoride (PVDF) membrane (Roche Applied Science, USA), and probed with indicated antibodies, respectively. The IgG secondary antibody was used and the blots were developed using TMB immunoblotting system.

Hematoxylin–eosin staining

Tumor tissues were fixed overnight at 4°C in 4% paraformaldehyde, incubated in 30% sucrose and optical cutting temperature compound (OCT), frozen, and sectioned at 5 μm. Sections were stained with hematoxylin and eosin (H&E) and observed by fluorescence microscope at 200× magnification.

Ethics statement

Research reported in this manuscript was performed with the approval of the ethics committee of the second affiliated hospital of Soochow University. Animal studies were approved by the Soochow University Animal Care and Use Committee, and they followed internationally recognized guidelines. Animals were euthanized by slow (20%/minute) displacement of chamber air with compressed CO_2 delivered through a precision flowmeter. The animals were subjected to cervical dislocation as a secondary means to ensure death. All efforts were made to minimize suffering. Details of the animal welfare and steps taken to ameliorate suffering were in accordance with the Regulations for the Administration of Affairs Concerning Experimental Animals approved by the State Council of the People's Republic of China.

Statistical analysis

All data were expressed as means ± SEM. Statistical analyses were performed by one-way ANOVA followed by Bonferroni's posttest for multiple comparisons. The statistical analyses were performed using the (SPSS 19.0, USA) software package. $P < 0.05$ was considered to be statistically significant.

Results

Survival status, tumor volume, and weight of the tumor-bearing mice

During the experiment, dietary habits, defecation patterns, and daily activities of the animals were normal, and no accidental deaths occurred. Weight gain or loss in each group was not obvious (Table 1); and the peripheral

Table 1. Evaluation of drug toxicity based on the body weight change.

Group	IBW	FBW	FBW/IBW
Control	18.50 ± 0.95	24.17 ± 1.33	1.3
HBOT	18.32 ± 0.60	23.94 ± 2.92	1.31
ACNU	17.94 ± 0.40	20.18 ± 0.93	1.12
HBOT+ACNU	18.07 ± 0.32	19.95 ± 1.62	1.1

The mice were divided into the four groups randomly: control group (untreated), hyperbaric oxygen therapy (HBOT) (only), nimustine (ACNU) (only), and HBOT+ACNU (combination), and each group had five mice, as shown in the Material and Methods section.

hemogram related to ACNU treatment induced no corresponding clinical symptoms, although white blood cell count was reduced from pretherapeutic 15.0×10^9/L to posttherapeutic 3.83×10^9/L, which was revealed to be reversible in the following review. According to the tumor length and short diameter measured by a caliper, tumor volume was converted and tumor growth curve was drawn, which demonstrated that the tumor growth rate reduced in the four groups, successively. The starting time of negative acceleration in the proliferation rate reflected by the curve showed an observable initiation in the D group (HBOT+ACNU combination) 16 days after inoculation. In addition, the C group (ACNU treatment) presented an initial negative acceleration in proliferation rate 22 days after inoculation. In contrast, the proliferation rate of the B group (HBOT treatment) and the A group (control) was nearly the same, while the absolute volume and mass were smaller in the B group than those of the A group.

At the end of the experiment, the whole tumor tissues were extracted completely, the tumor mass was weighed, and the tumor volume was measured by a caliper, demonstrating that differences in tumor mass, volume, and proliferation curve among four groups showed consistent general trends (Fig. 2A). The tumor mass was 6.03 ± 1.47 g, 4.13 ± 1.82 g, 2.39 ± 0.25 g, and 1.43 ± 0.38 g in A, B, C, and D groups, respectively ($P < 0.05$, Group B vs. A; $P < 0.01$, Group C or D vs. A). On the other hand, the tumor weights in D group were significantly smaller than those in both B and C groups (both $P < 0.05$). But it was not statistically significant between B group and C group ($P > 0.05$, Fig. 2B).

We also compared the tumor inhibition rate across the four groups. We found that tumor inhibition rate was 31.51%, 43.79%, and 76.29% in the B, C, and D groups, respectively. We tested if the ACNU and HBOT combination showed synergism based on Jin's formula $Q = Ea + b/(Ea + Eb - Ea \times Eb)$, where Ea + b, Ea, and Eb are the average effects of the combination treatment, and $Q < 0.85$ indicates antagonism, $0.85 \le Q < 1.15$ indicates additivity, and $Q \ge 1.15$ indicates synergism [11]. Our Q value was 1.24, indicating ACNU, and combination treatment showed synergistic effect.

Tumor tissue pathology and inflammatory cell infiltration analysis

H&E staining showed that tumors in the control group presented invasive growth, apparent cell heteromorphism, nuclear hyperchromatism, and abundant blood vessels, and the necrosis and hemorrhage were quite common, which were in line with the essential characteristics of the SU3 subcutaneous transplantation tumor, previously reported by our group [12]. In contrast, the necrosis and hemorrhage were reduced significantly in the HBOT and ACNU groups, especially in the HBOT+ACNU combined treatment group, which showed no necrotic or hemorrhagic foci basically, loosely arranged cells, significantly reduced interstitial components, and solid tumor. Moreover, in the control group, necrotic foci were detected under a white light microscope, while host-derived green inflammatory cell infiltration was found under a fluorescence microscope in the same H&E-stained section, and infiltration area was in accordance with necrotic foci (Fig. 3). Furthermore, total green fluorescence intensity was analyzed, using Image-Pro Plus6.0 (Silver Spring, USA) medical images. With the A group as basal level (1, 100%), the ratios of the groups B, C, and D were 0.44 ($P < 0.05$), 0.29 ($P < 0.05$), and 0.15 ($P < 0.05$), respectively. These results demonstrated that the degree of necrosis was reduced, and inflammatory cell infiltration also decreased

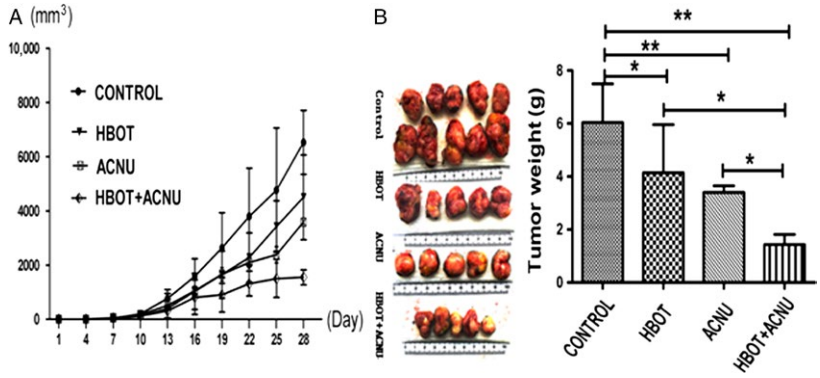

Figure 2. The tumor volume and weight of the tumor-bearing mice. (A) A comparison of the proliferation rates of transplanted tumors in different groups: proliferation rates in the control group, the hyperbaric oxygen therapy (HBOT) group, the nimustine (ACNU) group, and the HBOT+ACNU group reduced in turn. (B) Comparison of tumor mass in different groups. *$P < 0.05$, **$P < 0.01$. The mice were divided into the four groups randomly, and each group had five mice, as shown in the Material and Methods section.

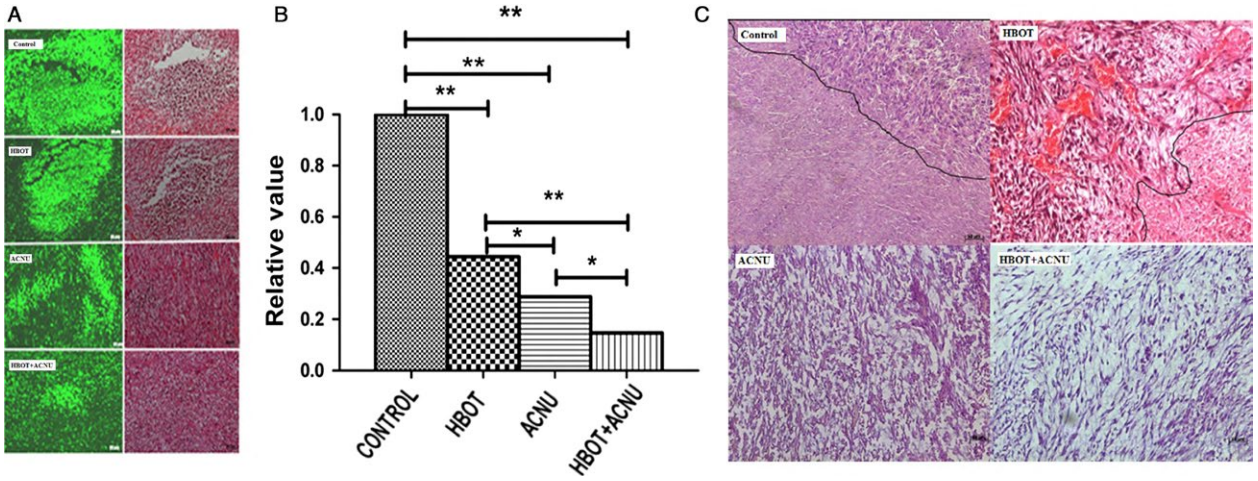

Figure 3. Observation of host cell infiltration (green) in necrotic tumor tissue and H&E-stained transplanted tumors. (A) Host cell infiltration (green) in necrotic tumor tissue under a microscope. One H&E-stained tissue section under fluorescent light and white light of a fluorescent microscope. The numbers of infiltrating cells with green fluorescence were different between the groups due to various sizes of necrotic areas; (B) for host cell infiltration (green) in necrotic tumor tissue, the relative ratios of the total intensity of green fluorescence in the control group to those in the other groups measured by Image-Pro Plus 6.0 software. (C) H&E-stained transplanted tumors under an optical microscope. The control group: necrotic areas with unclear tissue structure on the bottom left of the figure and non-necrotic areas on the upper right, with a compact oncocytes arrangement, deeply stained nucleus, and distinct morphological changes. The hyperbaric oxygen therapy (HBOT) group: necrotic areas with unclear tissue structure on the bottom right of the figure and non-necrotic areas on the upper left, with a compact oncocytes arrangement, deeply stained nucleus, distinct morphological changes, and many blood vessels. It was hard to determine necrotic areas in the nimustine (ACNU) group and the HBOT+ACNU group under an optical microscope. The cell arrangement of non-necrotic areas was looser in the ACNU group than in the HBOT+ACNU group. The scale bar: 20×. The mice were divided into the four groups randomly, and each group had five mice, as shown in the Material and Methods section. $*P < 0.05$; $**P < 0.01$

after both HBOT and ACNU treatments. Additionally, these clinical phenotypes were consistent with the changes in tumor volume and tumor mass, with the D group presenting the most obvious phenotypes and changes.

Molecular regulatory molecules analysis

Since inflammation plays an important role in tumor development, which mainly acts through the medium of a number of inflammatory cytokines, such as IL-1β and TNF-α. Abnormal expression of these factors as well as other carcinogenic factors, such as NF-κB and MMP9, further promotes tumor progression. Therefore, we further investigated the affect of hyperbaric oxygen on the expression of IL-1, TNFα, and other factors including HIF-1α, NF-κB, VEGF, and MMP9, which were closely related to tumor development.

The expression of the molecules, including TNF-α, IL-1β, HIF-1α, NF-κB, VEGF, and MMP9 in tumor tissues was analyzed by the methods of immunohistochemistry and western blot. The results of sections were shown in Table 2 and Figure 4. The quantity of all six molecules in tumor tissues from HBOT+ACNU (combination) group and HBOT (only) group were efficiently attenuated, compared with that of control (untreated) group and ACNU (only) group, suggesting HBOT could effectively inhibit the expression of six molecules. The HBOT–ACNU treatment induced molecular regulation network combined with KEGG database data, using Pathway Builder software, as were illustrated in Figure 5, showing that HBO increased the sensitivity of ACNU against glioma by regulating HIF–TNF–NF-κB signaling pathway.

Discussion

Tumor tissue hypoxia and HBOT

The presence of tumor tissue hypoxia had become an unquestioned fact. It was found that hypoxia of high-grade glioma was severe than that of low-grade glioma, and hypoxia could promote rather than inhibit tumor growth [13–15]. Our team had proved that glioma stem cells could transform into tumor vascular endothelial cell under low PO_2 condition, and one of the reasons for low PO_2-promoting tumor growth was that reconstructed tumor vessels directly participated in tumor blood circulation [16, 17]. If HBOT truly enhanced PO_2 in tumor tissues, then the above-mentioned debate on HBOT of malignant tumor might arrive at the same conclusion. Therefore, PO_2 in tumor tissues must be monitored during HBOT experiments on tumor-bearing animals, to avoid the situation, in which the tumor tissue PO_2 was not enhanced owing to some reasons from HBOT itself.

Table 2. Comparison of associated molecular protein in different groups (mean optical density).

Group	HIF-1α	NF-κB	VEGF	MMP9	TNF-α	IL-1β
ACNU	0.067 ± 0.012	0.046 ± 0.006	0.021 ± 0.004	0.031 ± 0.006	0.076 ± 0.006	0.027 ± 0.001
HBOT	0.016 ± 0.005	0.003 ± 0.001	0.016 ± 0.008	0.005 ± 0.003	0.005 ± 0.003	0.006 ± 0.003
HBOT+ACNU	0.011 ± 0.005	0.001 ± 0.001	0.008 ± 0.003	0.003 ± 0.002	0.003 ± 0.001	0.003 ± 0.005
Control	0.069 ± 0.014	0.05 ± 0.014	0.049 ± 0.018	0.039 ± 0.001	0.0104 ± 0.02	0.03 ± 0.007

The mice were divided into the four groups randomly: control group (untreated), HBOT (only), nimustine (ACNU) (only), HBOT+ACNU (combination), and each group had five mice, as shown in the Material and Methods section.

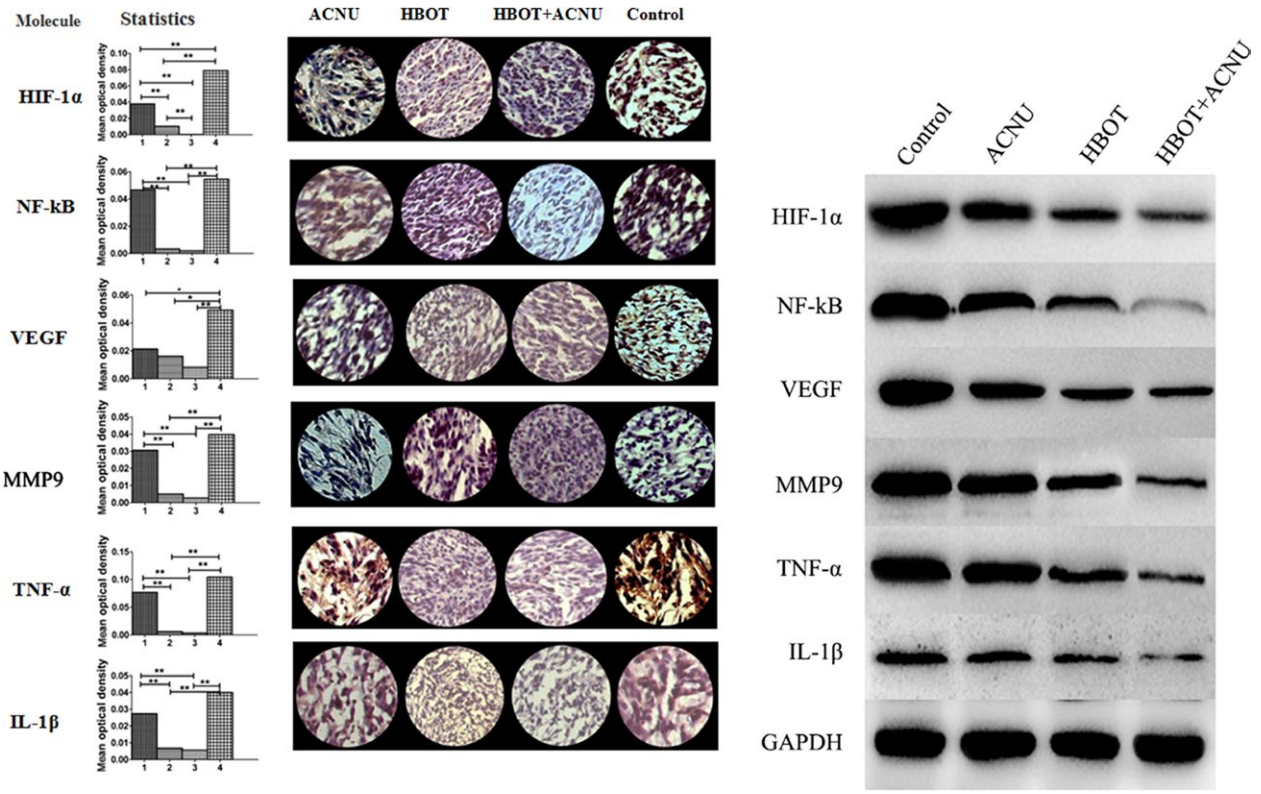

Figure 4. Statistical chart of the gray values obtained from immunohistochemical analysis of relevant proteins in hyperbaric oxygen therapy (HBOT) combined with nimustine (ACNU) therapy. The left side showed the gray values; the middle part showed immunohistochemically stained samples under a microscope (40×); the right side showed expression levels of HIF-1α, TNF-α, IL-1β, VEGF, MMP9, and NF-κB, using western blotting method, with endogenous GAPDH as internal control. The *x*-axis of the histogram showed the ACNU group (1), the HBOT group (2), the HBOT+ACNU group (3), and the control group (4), respectively; the *y*-axis indicated mean optical density. The mice were divided into the four groups randomly, and each group had five mice, as shown in the Material and Methods section. $*P < 0.05$; $**P < 0.01$

Otherwise, the discussion on the efficacy of HBOT would lack the most basic evidence. Kayama et al. [18] directly measured oxygen pressure (PO_2) in tumor tissue, which was significantly lower than that in surrounding brain tissue. We determined PO_2 in the model of this experiment with unisense microelectrode, showing that PO_2 in the brain of mice treated with HBOT, was much higher than that in normal mouse, and that tumor tissue PO_2 was also enhanced and was getting close to that in normal mouse brain (Fig. 6).

Molecular regulatory pathways influenced by HBOT

We had previously reported that reversible malignant cell proliferation and necrotic tumor tissue in the present tumor model were related to high expression of HIF-1α, TNF-α, CD68, and CD11b [16, 17]. The control group in this study was a copy of the model, with not only HIF-1α and TNF-α, but also IL-1β, VEGF, MMP9, and NF-κB being highly expressed. However, their expression

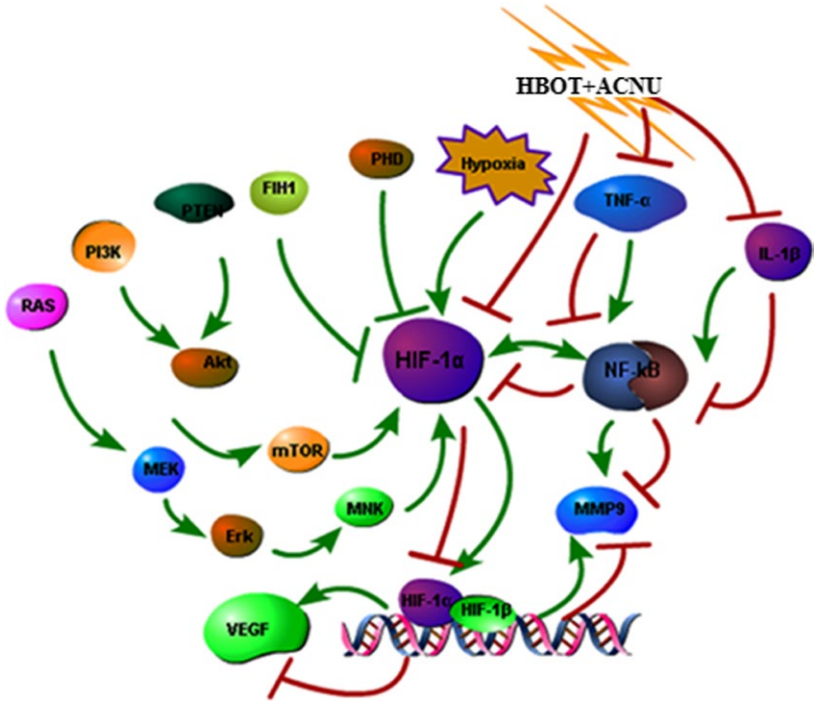

Figure 5. Diagram of hyperbaric oxygen therapy-induced HIF–TNF–NF-κB regulatory network.

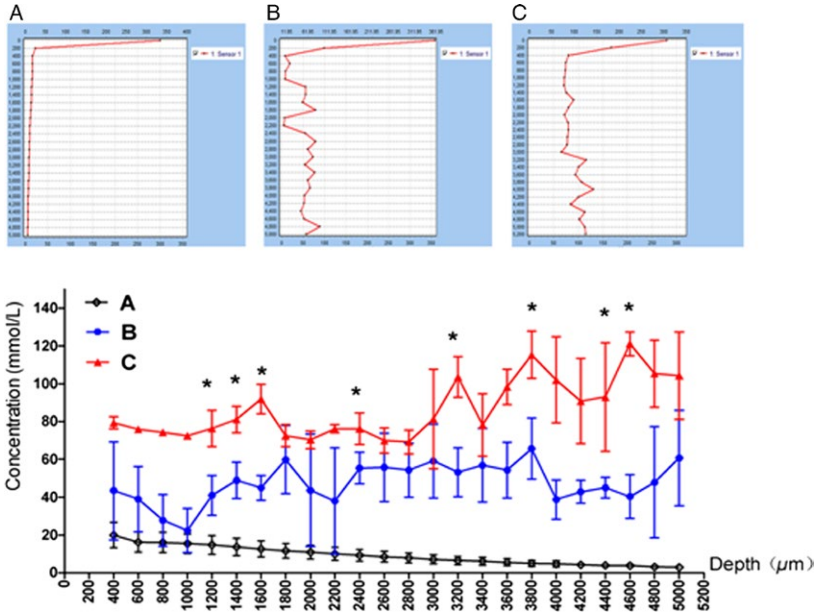

Figure 6. Determination of oxygen content in brain of rats after hyperbaric oxygen therapy (HBOT) by microelectrode. The vertical coordinate was oxygen concentration (mmol/L) and the horizontal coordinate was the probe into the depth of brain tissue (mm).*$P < 0.05$. The mice were divided into the four groups randomly, and each group had five mice, as shown in the Material and Methods section.

was reduced by HBOT to inhibit tumor proliferation. This had become a molecular evidence for effectiveness of HBOT on glioma and sensitizing effect of HBOT on ACNU, but its regulatory pathway still needed to be illuminated. Together with the data from KEEG database, we believed that the above six molecules basically covered

the sources of tumor and inflammatory cell, while nonresolving inflammation was the major cause of almost all malignant tumors [19]. Highly expressed inflammatory factors such as IL-1β and TNF-α, markers of inflammatory cells such as CD68 and CD11b, and massive inflammatory cells tracked by fluorescence in necrotic tumor tissue were detected in the tumor tissue of this model (Fig. 3). It suggested that this model was a copy of glioma and the genesis and progression of glioma were closely connected to nonresolving inflammation. Hypoxia-inducible factor (HIF) reported by Kumar and Gabrilovich [20] was one of the biggest concerns, as it was upregulated in cell responses to low PO_2, and this promoted immunosuppressive activity of nonresolving inflammatory cells such as MDSC (myeloid-derived suppressor cells) and TAM (tumor-associated macrophages) and accelerated transformation from MDSC into TAM.

TNFα, IL-1β, and NF-κB are also related to nonresolving inflammation. TNF includes TNF-α and β, which are generated by macrophage and lymphocyte, respectively. As a double-edged sword, TNF not only could induce tumor cell apoptosis [21] and enhance immune function [22], but also could induce expression of VEGF, MMPs, and sVCAM-1, and promote angiogenesis and tumor cell metastasis [23, 24]. IL-1 mainly includes IL-1α and IL-1β. IL-1β is widely expressed. Besides macrophages and monocytes, it had been reported by Tarassishin et al. [25] that glioma cells also had high expression of IL-1β. Immunological homeostasis maintains an absent or low expression of IL-1β, which could only be upregulated by stimulation of inflammatory signals [26, 27]. Large-dose IL-1β promotes expression of IGF/HGF, MMPs, MCAM, VEGF, and NLRP3, and played a role in tumor angiogenesis, cell invasion, and dispersion [25, 28–30].

In conclusion, HBOT could inhibit glioma cell proliferation and inflammatory cell infiltration, and also exerted a sensitizing effect on ACNU therapy. This was associated with the fact that HBOT enhanced PO_2 in tumor tissues and thus leaded to low expression of HIF-1α, TNF-α, IL-1β, VEGF, MMP9, and NF-κB. Therefore, hyperbaric oxygen therapy might be a potentially effective therapeutic option and might improve the prognosis for patients with glioma. The combination of hyperbaric oxygen with ACNU therapy produced an important reduction in glioma growth and effective approach to the treatment of glioblastoma.

Acknowledgments

This study was supported by grants from the National Natural Science Foundation (81472739, 81572480, 81172400), the Natural Science Foundation of Jiangsu China (BK20151214), and the Suzhou Science and Technology Development Program (SYS201507).

Conflict of Interest

The authors declare no conflict of interest.

References

1. Yan, L., T. Liang, and O. Cheng. 2015. Hyperbaric oxygen therapy in China. Med. Gas Res. 5:3.
2. Wenwu, L., S. Xuejun, T. Hengyi, and L. Kan. 2013. Hyperbaric oxygen and cancer: more complex than we expected. Target Oncol. 8:79–81.
3. Moen, I., and L. E. Stuhr. 2012. Hyperbaric oxygen therapy and cancer–a review. Target Oncol. 7:233–242.
4. Stuhr, L. E., A. Raa, M. Oyan, et al. 2007. Hyperoxia retards growth and induces apoptosis, changes in vascular density and gene expression in transplanted gliomas in nude rats. J. Neurooncol. 85:191–202.
5. Takiguchi, N., N. Saito, M. Nunomura, et al. 2001. Use of 5-FU plus hyperbaric oxygen for treating malignant tumors: evaluation of antitumor effect and measurement of 5-FU in individual organs. Cancer Chemother. Pharmacol. 47:11–14.
6. Petre, P. M., F. A. Baciewicz, S. Tiqan, et al. 2003. Hyperbaric oxygen as a chemotherapy adjuvant in the treatment of metastatic lung tumors in a rat model. J. Thorac. Cardiovasc. Surg. 125:85–95.
7. Randal, C., M. D. Paniello, L. Patrick, et al. 2013. Effect of hyperbaric oxygen therapy on a murine squamous cell carcinoma model. Head Neck 36:1743–1746.
8. Shewell, J., and S. C. Thompson. 1980. The effect of hyperbaric oxygen treatment on pulmonary metastasis in the C3H mouse. Eur. J. Cancer 16:253–259.
9. Wan, Y., X. F. Fei, Z. M. Wang, et al. 2012. Expression of miRNA-125b in the new, highly invasive glioma stem cell and progenitor cell line SU3. Chin J. Cancer. 31:207–214.
10. Dong, J., X. L. Dai, Z. H. Lu, et al. 2012. Incubation and application of transgenic green fluorescence nude mice in visualization studies on glioma tissue remodeling. Chin. Med. J. (Engl) 125:4349–4354.
11. Huang, H. Y., J. L. Niu, and Y. H. Lu. 2012. Multidrug resistance reversal effect of DMC derived from buds of *Cleistocalyx operculatus* in human hepatocellular tumor xenograft model. J. Sci. Food Agric. 92:135–140.
12. Zhaohui, L., L. Ke, Z. Jinshi, et al. 2014. Establishment of green fluorescent protein tracing murine model focused on the functions of host components in necrosis repair and niche of subcutaneously implanted glioma. Oncol. Rep. 31:654–661.
13. Thomlinson, R. H., and L. H. Gray. 1955. The histological structure of some human lung cancers and the possible implications for radiotherapy. Br. J. Cancer 9:539–549.

14. Collingadge, D. R., J. M. Piepmeier, S. Rockwell, et al. 1999. Polarographic measurements of oxygen tension in human glioma and surrounding peritumoural brain tissue. Radiother. Oncol. 53:127–131.
15. Nordgren, I. K., and A. Tavassoli. 2011. Targeting tumour angiogenesis with small molecule inhibitors of hypoxia inducible factor. Chem. Soc. Rev. 40:4307–4317.
16. Zhao, Y., J. Dong, Q. Huang, et al. 2010. Endothelial cell transdifferentiation of human glioma stem progenitor cells in vitro. Brain Res. Bull. 82:308–312.
17. Dong, J., Y. D. Zhao, Q. Huang, et al. 2011. Glioma stem/progenitor cells contribute to neovascularization via transdifferentiation. Stem Cell Rev. Rep. 7:141–152.
18. Kayama, T., T. Yoshimoto, S. Fujimoto, et al. 1991. Intratumoral oxygen pressure in malignant brain tumor. J. Neurosurg. 74:55–59.
19. Carl, N., and D. Aihao. 2010. Nonresolving inflammation. Cell 140:871–882.
20. Kumar, V., and D. I. Gabrilovich. 2014. Hypoxia-inducible factors in regulation of immune responses in tumour microenvironment. Immunology 143:512–519.
21. Lyu, M. A., and M. G. Rosenblum. 2005. The immunocytokine scFv23/TNF sensitizes HER-2/neu-overexpressing SKBR-3 cells to tumor necrosis factor (TNF) via up-regulation of TNF receptor-1. Mol. Cancer Ther. 4:1205–1213.
22. Ebert, L. M., S. Meuter, and B. Moser. 2006. Homing and function of human skin gamma delta T cells and NK cells: relevance for tumor surveillance. J. Immunol. 176:4331–4336.
23. Warren, M. A., S. F. Shoemaker, D. J. Shealy, et al. 2009. Tumor necrosis factor deficiency inhibits mammary tumorigenesis and a tumor necrosis factor neutralizing antibody decreases mammary tumor grow thin neu/erbB2 transgenic mice. Mol. Cancer Ther. 8:2655–2663.
24. Yin, Y., X. Chen, and Y. Shu. 2009. Gene expression of the invasive phenotype of TNF-alpha-treated MCF-7 cells. Biomed. Pharmacother. 63:421–428.
25. Tarassishin, L., D. Casper, and S. C. Lee. 2014. Aberrant expression of interleukin-1β and inflammasome activation in human malignant gliomas. PLoS ONE 9:e103432.
26. Voronov, E., Y. Carmi, and R. N. Apte. 2007. Role of IL-1 mediated inflammation in tumor angiogenesis. Adv. Exp. Med. Biol. 601:265–270.
27. Lewis, A. M., S. Varghese, H. Xu, et al. 2006. Interleukin-1 and cancer progression: the emerging role of interleukin-1 receptor antagonist as a novel therapeutic agent in cancer treatment. J. Transl. Med. 4:48–59.
28. Lee, C. H., J. S. Chang, S. H. Syu, et al. 2015. IL-1β promotes malignant transformation and tumor aggressiveness in oral cancer. J. Cell. Physiol. 230:875–884.
29. Carmi, Y., S. Dotan, P. Rider, et al. 2013. The role of IL-1β in the early tumor cell-induced angiogenic response. J. Immunol. 190:3500–3509.
30. Apte, R. N., and E. Voronov. 2008. Is interleukin-1 a good or bad 'guy' in tumor immunobiology and immunotherapy? Immunol. Rev. 222:222–241.

